On the Energy Consumption and Ranging Accuracy of Ultra-Wideband Physical Interfaces

Laura Flueratoru*†, Silvan Wehrli‡, Michele Magno§ and Dragoș Niculescu*
* Computer Science Department, University Politehnica of Bucharest, Romania
† Electrical Engineering Unit, Tampere University, Finland
‡3db Access AG, Zürich, Switzerland
§ Department of Information Technology and Electrical Engineering, ETH Zürich, Switzerland

GLOBECOM 2020 - 2020 IEEE Global Communications Conference | 978-1-7281-8298-8/20/$31.00 ©2020 IEEE | DOI: 10.1109/GLOBECOM42002.2020.9347984

***Abstract*—Ultra-wideband (UWB) communication is attracting increased interest for its high-accuracy distance measurements. However, the typical current consumption of tens to hundreds of mA during transmission and reception might make the technology prohibitive to battery-powered devices in the Internet of Things. The IEEE 802.15.4 standard specifies two UWB physical layer interfaces (PHYs), with low- and high-rate pulse repetition (LRP and HRP, respectively). While the LRP PHY allows a more energy-efficient implementation of the UWB transceiver than its HRP counterpart, the question is whether some ranging quality is lost in exchange. We evaluate the trade-off between power and energy consumption, on the one hand, and distance measurement accuracy and precision, on the other hand, using UWB devices developed by Decawave (HRP) and 3db Access (LRP). We find that the distance measurement errors of 3db Access devices have at most $12\,\mathrm{cm}$ higher bias and standard deviation in line-of-sight propagation and 2–3 times higher spread in non-line-of-sight scenarios than those of Decawave devices. However, 3db Access chips consume 10 times less power and 125 times less energy per distance measurement than Decawave ones. Since the LRP PHY has an ultra-low energy consumption, it should be preferred over the HRP PHY when energy efficiency is critical, with a small penalty in the ranging performance.**

***Index Terms*—Ultra-Wideband (UWB), Distance Measurement, Accuracy, Energy Efficiency**

I. Introduction

Ultra-wideband (UWB) radio frequency (RF) signals have a high time resolution which enables the precise timestamping of their reception. As a result, they can provide time-of-flight (ToF) measurements with sub-nanosecond accuracy which can be further converted into distance and location information with cm- or dm-level accuracy [1], [2]. Location awareness can augment the capabilities of devices in the Internet of Things (IoT) and is often used in wireless sensor networks, industrial processes, or health-related applications. UWB devices usually consume tens to hundreds of mA, making them fit for localization tasks on energy-constrained devices. Their popularity has therefore risen and they have been recently included in smartphones [3], facilitating their large-scale deployment on the consumer market. Moreover, enhancements to the ranging capabilities of UWB devices are currently being developed by the IEEE 802.15.4z Enhanced Impulse Radio (EIR) Task Group [4]. An overview of the enhancements to the IEEE 802.15.4 standard proposed by the EIR Task Group 4z can be found in [5].

The IEEE Standard for Low-Rate Wireless Networks 802.15.4 [6] specifies two UWB physical interfaces (PHYs), that use that use high- and low-rate pulse repetition (HRP and LRP, respectively). Transmitting pulses at low rates means that a single pulse can have the highest energy under UWB regulations [7]. The high instantaneous pulse amplitude enables the implementation of LRP PHYs with non-coherent receivers which are more energy-efficient than coherent ones. If we increase the pulse rate, we must decrease the energy per pulse, causing link budget losses which can be compensated by coherent pulse integration [8].

The LRP PHY, therefore, can be implemented with a more energy-efficient transceiver design than the HRP PHY, suitable for low-complexity active RFID tags. Coherent and non-coherent architectures have been compared from a theoretical standpoint in [9] and the authors found that the latter typically have an SNR loss of at least $5\,\mathrm{dB}$ but better multipath, phase jitter, and synchronization characteristics than the former.

The effect of LRP and HRP PHYs on distance measurement quality has not yet been evaluated. Previous work has focused mostly on the ranging accuracy of UWB devices [10]–[12] — most often, the Decawave DW1000 IC [13], which implements the HRP PHY — or on integrating UWB devices in localization systems [1], [2]. Comparisons of UWB devices have evaluated only the distance measurement accuracy, without regards to the power and energy consumption [14]–[16]. Moreover, only one of them has included an LRP PHY device (developed by Ubisense) [14].

To the best of our knowledge, we are the first to compare the distance measurements and power and energy consumption of LRP and HRP devices. To quantify the trade-off between energy consumption and ranging quality, we perform measurements using two commercially-available UWB devices: the Decawave DW1000 IC (HRP) and the 3db Access 3DB6830C IC [17] (LRP)[1].

The main contributions of this paper are the following:

The authors gratefully acknowledge funding from European Union's Horizon 2020 Research and Innovation programme under the Marie Skłodowska Curie grant agreement No. 813278 (A-WEAR: A network for dynamic wearable applications with privacy constraints, http://www.a-wear.eu/).

[1]We will refer to the 3db 3DB6830C (Release 2016) and the Decawave DW1000 (Release 2014) as the 3db and Decawave ICs, respectively.

978-1-7281-8298-8/20/$31.00 ©2020 IEEE

- We measure the average power consumption of the chosen devices in the receive, transmit, and idle modes and compute their energy consumption per ranging.
- We compare the channel impulse responses (CIRs) of 3db and Decawave devices acquired in identical settings, which are essential to understand the distance estimation.
- We compare the range of 3db and Decawave devices.
- We conducted an extensive distance measurement campaign with 3db devices in indoor multipath environments. We compare our ranging results with already-published results on Decawave devices [10]–[12], [15]. We classify distance measurement errors based on whether they were acquired in line-of-sight (LOS) propagation, with no obstruction between the transmitter and the receiver, or non-line-of-sight (NLOS) propagation, when an object blocks the direct path.

II. Device Characteristics

Decawave devices are compliant with the HRP PHY defined in the IEEE 802.15.4a amendment, now part of the main standard [6]. They are the most widely-used UWB devices, which is why we chose them to represent the HRP PHY class. The 3db IC is compliant with the LRP PHY specified in the upcoming IEEE 802.15.4z amendment [4]. The chip is already used for secure keyless car access but it has not been evaluated in high-accuracy applications so far.

In this section, we study how Decawave and 3db devices differ in terms of pulse repetition frequency, receiver architecture, and ranging methods in Sections II-A, II-B, and II-C, respectively. We also highlight how their characteristics affect the power consumption and distance measurement accuracy.

A. High- and Low-Rate Pulse Repetition

UWB transmissions have to satisfy two constraints imposed by international regulations [18]: a maximum *average* power spectral density (PSD) of $-41.3\,\mathrm{dBm/MHz}$ (averaged over $1\,\mathrm{ms}$) and a maximum *peak* power spectral density of $0\,\mathrm{dBm/50MHz}$. UWB devices can therefore transmit over a fixed period of time either few pulses at high power levels or a large number of pulses with lower transmit power. The first situation falls under the LRP specification and is employed by 3db devices, while the latter is known as HRP and is used by Decawave. If optimally employed, both of these technologies benefit from an *equal* average transmitted RF energy.

Since the HRP PHY transmits individual pulses with lower energy than the LRP, the received pulse energy is also lower for the same path loss (same distance). Therefore, the HRP PHY needs more sophisticated techniques to extract weaker pulses from the receiver noise, typically performed with correlations over a large number of samples.

B. Device Architecture

Owing to the LRP PHY, 3db devices can be implemented with a *non-coherent* receiver based on energy detection (ED) for signals modulated with binary frequency-shift keying (BFSK). This signaling scheme allows the circuitry implementation of the receiver to be more energy efficient than the *coherent* Decawave receiver.

Coherent receivers have low sensitivity to inter-symbol and co-user interference and benefit from the multipath diversity of the UWB channel [19]. At the same time, the receiver architecture demands high computational resources and hardware complexity [20]. For optimal reception, the coherent receiver needs to estimate the multipath delays, their channel coefficients, and the pulse shape distortion [20]. Precisely estimating the carrier phase is crucial for recovering the baseband pulse, since inaccuracies will result in signal power loss and crosstalk interference in PSK-modulated signals [21]. For a carrier frequency of $8\,\mathrm{GHz}$, a time shift of half of the pulse period flips the phase of the signal, so coherent UWB systems generally tolerate rotations only within $\pi/4$ of the signal phase (around $30\,\mathrm{ps}$). These requirements increase the power consumption of coherent demodulators [19].

Non-coherent receivers estimate channel coefficients based on the envelope rather than the phase and amplitude of the received signal, relaxing synchronization constraints. The timing requirements of a non-coherent receiver are dependent only on the pulse envelope, which is related to the pulse bandwidth. For instance, if the pulse bandwidth is $500\,\mathrm{MHz}$, the non-coherent receiver needs to operate with a timing resolution of $1\,\mathrm{ns}$ and does not need sophisticated RF carrier synchronization. Therefore, non-coherent receivers can be more energy-efficient albeit with a higher bit error probability in comparison with the coherent architecture [21].

C. Ranging Methods

A popular application for UWB devices is indoor localization. Owing to the high time resolution of UWB signals, time-based localization techniques are the most suitable for UWB devices [22]. In this paper, we chose to compare the *ranging* accuracy and precision of the UWB devices instead of the *localization* ones for several reasons. First, many popular localization algorithms (e.g. trilateration) work directly with distance estimates between the tracked device (tag) and the reference devices (anchors), so our results can be used to compute the expected localization accuracy of those algorithms. Second, localization results are heavily influenced by factors unrelated to the devices themselves, such as the anchor placement, the location of the tag[2], or the localization algorithm. Since we are interested in comparing the devices themselves, it is easier to avoid these effects by evaluating the ranging performance instead of the localization one. Third, there are important applications of UWB devices which do not involve localization, such as keyless car access and, in the future, possibly contact tracing, so our results can be used to evaluate which physical interface is more suitable for them.

The distance between two devices can be estimated based on the time of flight (ToF) of the signal. If we know the

[2]Localization errors are larger near the anchors and lower in the center of the tracking area [23].

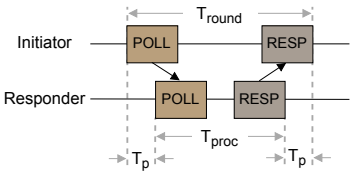

(a) SS-TWR

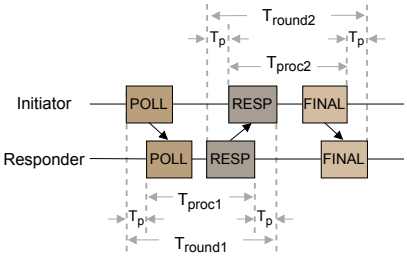

(b) DS-TWR

Fig. 1: Message exchange in the single- and double-sided two-way ranging which are the ranging methods of choice for the LRP and HRP PHYs, respectively.

transmission time (T_1) of the signal measured by the sender and the arrival time (T_2) at the receiver, we can compute the distance as:

$$d = (T_2 - T_1) \cdot c, \tag{1}$$

where c is the speed of light and $T_p \triangleq T_2 - T_1$ is the propagation time of the signal. To accurately estimate the distance, the devices need to be tightly clock synchronized, as a small mismatch of $1\,\mathrm{ns}$ can introduce a distance error of around $30\,\mathrm{cm}$. Because synchronizing the sender and the receiver is usually unfeasible in practice, more messages are exchanged in order reduce such errors, leading to the single- and the double-sided two-way ranging.

Single-Sided Two-Way Ranging (SS-TWR): The SS-TWR uses two messages per distance estimate, as shown in Fig. 1a. The propagation time is:

$$T_p = \frac{T_{round} - T_{proc}}{2}, \tag{2}$$

where T_{round} is the time spent in one message exchange and T_{proc} is the processing time on the responder side. It can be shown that the error in estimating T_p is [24]:

$$e_{T_p} = e_1 \cdot T_p + \frac{1}{2} T_{proc}(e_1 - e_2), \tag{3}$$

where e_1 and e_2 are the clock drift errors of the initiator and responder, respectively. The main source of errors in the SS-TWR are T_{proc}, which is in the range of hundreds of microseconds, and the clock drift, which can be up to $\pm 20\,\mathrm{ppm}$ in systems compliant with the IEEE 802.15.4 standard [6].

In the LRP PHY, a location-enhancing information postamble is introduced at the end of each message to estimate the clock drift error [6]. In addition, the processing time of LRP messages is shorter than the one of HRP. It is also more convenient to minimize the number of exchanged messages in the TWR since this reduces the time needed to obtain one

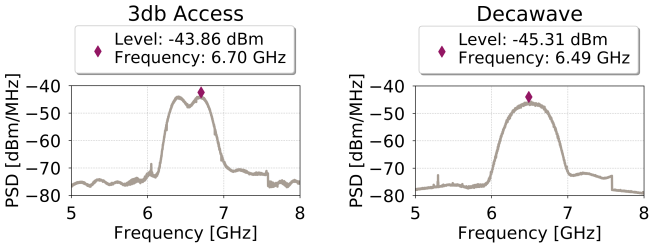

Fig. 2: The power spectral density of 3db and Decawave ICs.

distance measurement. Therefore, the SS-TWR is usually the method of choice for LRP devices.

Double-Sided Two-Way Ranging (DS-TWR): Because the HRP PHY does not include a postamble, it needs another method to minimize clock drift errors. This can be achieved by exchanging an additional message, as shown in Fig. 1b, leading to the DS-TWR. In this case, e_{T_p} is minimized *if* the processing times T_{proc1} and T_{proc2} are equal. However, this constraint is often hard to enforce in practice. An alternative DS-TWR has been proposed which minimizes clock drift errors even with asymmetric processing times [24]. This is the method currently used by Decawave [13].

III. Evaluation Setup

To evaluate how the system architecture influences the power consumption and distance measurements, we implement the ranging techniques on 3db and Decawave hardware. In the following, we describe the device setups.

3db Access: We integrate the 3db chip in an Arduino shield on top of an Arduino M0 board. The communication between the chip and the host MCU is performed via SPI. We use the lowest channel, centered at $6.52\,\mathrm{GHz}$, and a peak data rate of $247\,\mathrm{kb/s}$. The $10\,\mathrm{dB}$ bandwidth of a pulse is $380\,\mathrm{MHz}$ and, because pulse spectra partially overlap in BFSK modulation, the total system bandwidth is approximately $620\,\mathrm{MHz}$. The packet duration is $400\,\mu\mathrm{s}$.

Decawave: We use the Decawave EVB1000 evaluation boards, which include a software kit for ranging applications. We configure the devices to communicate on a similar center frequency as 3db ones, of $6.49\,\mathrm{GHz}$ (Channel 5), using a $3\,\mathrm{dB}$ bandwidth of $499.2\,\mathrm{MHz}$ (equivalent to a $10\,\mathrm{dB}$ bandwidth of $\approx 662\,\mathrm{MHz}$). We set a data rate of $110\,\mathrm{kb/s}$, a PRF of $16\,\mathrm{MHz}$, and a preamble length of 2048 symbols (Mode 3). The packet duration in this mode is $3487\,\mu\mathrm{s}$. The lower data rate allows longer range and increased link budget compared to higher-rate setups, while the PRF and preamble length were chosen to minimize NLOS effects.

The lower pulse bandwidth of 3db devices can, in theory, decrease the ranging precision, due to the lower time resolution. However, it is compensated by the frequency diversity added by the BFSK modulation.

Both ICs were configured to operate within UWB regulations, which specify a maximum transmit level of $-41.3\,\mathrm{dBm/MHz}$ [18]. Fig. 2 shows their measured power spectral densities (PSDs). The maximum transmit levels of

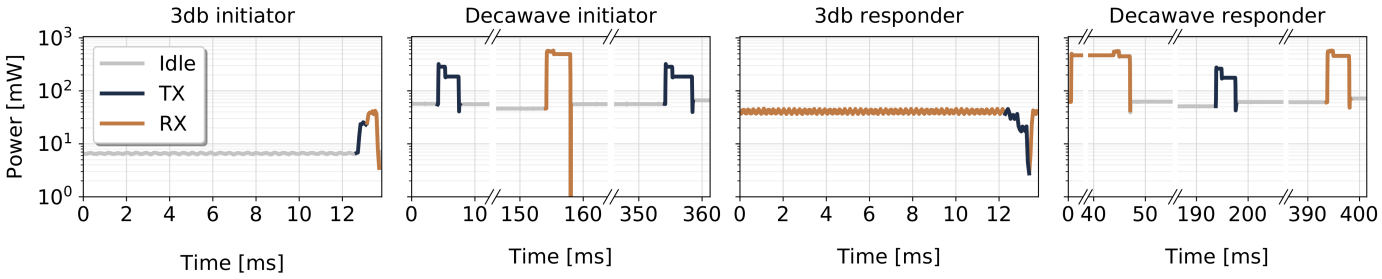

Fig. 3: The power consumption profiles of 3db and Decawave initiators and responders. The average power consumption of 3db devices is about 10 times lower than the one of Decawave devices in all modes (idle, transmission, reception).

TABLE I: The average power consumption of 3db and Decawave devices in the transmission (TX), reception (RX), and idle modes.

Device	Average power consumption [mW]		
	TX	RX	Idle
3db Access	20.69	40.70	6.60
Decawave	194.54	492.45	68.78

the DW1000 and the 3db IC are $-45.31\,\mathrm{dBm/MHz}$ and $-43.86\,\mathrm{dBm/MHz}$, respectively, but they do not include the antenna gain. The antenna gains of 3db and Decawave devices are $2\,\mathrm{dBi}$ and $3.3\,\mathrm{dBi}$ (at the center frequency), respectively, resulting overall in almost equal PSDs.

IV. Evaluation

In this section, we measure the average power consumption, channel impulse response (CIR), range, and distance measurement accuracy and precision of 3db and Decawave devices.

A. Power Consumption

We measured the current consumption of 3db and Decawave devices when performing the SS-TWR and DS-TWR, respectively, with a Keysight DC Power Analyzer. The 3db IC is powered with $1.25\,\mathrm{V}$ and the supply voltage of Decawave is $3.3\,\mathrm{V}$. We configured the 3db devices to perform one SS-TWR every approximately $14\,\mathrm{ms}$. The Decawave profile was obtained with the default firmware of the EVK1000 kit and the DecaRanging application which uses the DS-TWR method. Decawave recommends the use of guard times on the order of hundreds of ms between each message [25]. In our setup, Decawave devices perform one DS-TWR every $500\,\mathrm{ms}$.

Fig. 3 shows the power consumption of the 3db and Decawave initiators and responders (note the logarithmic y-axis). We isolate the receive (RX), transmit (TX), and idle modes and compute the average power consumption of each state, presented in Table I.

First, each device consumes more power in the RX mode than in the TX mode. Because of the large signal bandwidth, receivers need analog-to-digital converters (ADCs) operating at high sampling rates (on the order of $\mathrm{Gsamples/s}$). This increases the processing load at the receiver, demanding more energy consumption. The RX-to-TX average power consumption ratio is approximately 2 in the case of 3db devices and 2.5 in the case of Decawave.

Overall, the average power consumption of the 3db IC is 10 times lower than the one of the Decawave IC. Note that the average power consumption of Decawave devices in the *idle* mode is about $70\,\%$ higher than the one of 3db devices in the *receive* mode, also the most power-hungry state.

Besides these states, both devices have sleep modes which consume $1\,\mu\mathrm{A}$ (sleep) or 50–$100\,\mathrm{nA}$ (deep sleep) in the case of Decawave [13] and $500\,\mathrm{nA}$ in the case of 3db. When used together with the regular operational modes, they can increase the battery life of the device.

The power consumption profile is a starting point for evaluating the energy consumption of an UWB-based localization system (LS). A localization system (LS) consists of multiple, fixed devices with known positions (called anchors) which localize mobile devices (called tags). A key challenge is minimizing the energy consumption of the *tag*, which is usually battery-powered. To avoid synchronizing the tag and the anchors, the tag can *initiate* the message exchange and stay in the idle or sleep mode between rangings. Using the SS-TWR implies, in this case, that the *tag* estimates the distance (or the location). Alternatively, if the tag initiates a DS-TWR, the anchors are the last entities in the message exchange, so the *anchor* estimates the distance (or the location).

To illustrate the energy efficiency of a tag in a LS, let us consider the most favorable scenario for each device, in which the tag is the initiator. We disregard the time spent in the idle mode[3] and compute the energy consumption only when the device is in the TX or RX mode. Because the packet duration of the 3db chip is 10 times shorter than the one of Decawave, a 3db tag would consume $0.028\,\mathrm{mJ}$ per ranging, while a Decawave tag would need $3.55\,\mathrm{mJ}$. Therefore, a 3db tag can consume 125 less energy than a Decawave tag.

Decawave devices can indeed be more energy-efficient in the high-rate mode ($6.8\,\mathrm{Mb/s}$). In the best case, this allows a 20x shorter packet duration but about 1.4x higher current consumption [26]. So even in this mode the 3db IC consumes at least 9x lower energy, without taking into account the idle time. The $6.8\,\mathrm{Mb/s}$ mode also reduces the range, as we will see in Section IV-C.

[3]The time spent in the idle mode is subject to the desired location update rate and the chosen guard times. Since they can be chosen freely to a certain extent, we neglect them in the energy computation.

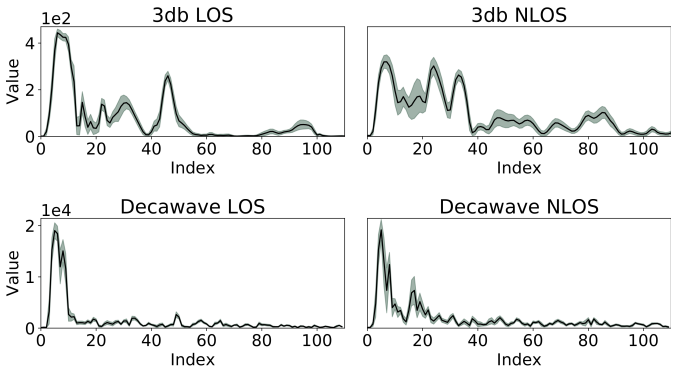

Fig. 4: Averaged CIRs and their path variations obtained by placing pairs of 3db and Decawave devices in LOS and NLOS of each other in exactly the same positions.

B. Channel Impulse Response

Time-based ranging methods precisely estimate the moment at which the signal is received. This corresponds to the leading edge (LE) of the first peak in the CIR. In the 3db IC, the CIR is obtained by directly integrating the pulse envelopes. The DW1000 IC estimates the CIR by accumulating over time the correlation of the received signal and a known preamble sequence [13]. Both CIRs have a sampling period of $1\,\mathrm{ns}$.

The measurement quality depends on how the signal propagates between the transmitter and the receiver. In the LOS scenario, there is a direct, unobstructed path between two devices, leading to minimal errors. In NLOS propagation, walls or large objects block the direct path and therefore attenuate or block the LOS signal. Copies of the signal reflected on surrounding objects might still reach the receiver, but the additional delay can introduce large ranging errors in NLOS scenarios. We should therefore distinguish between these two cases when analyzing data.

We conducted an experiment in which we placed pairs of 3db and Decawave devices in a LOS and a NLOS scenario, in exactly the same positions. In the NLOS case, a concrete pillar was blocking the direct path between the devices. We acquired approximately 150 CIR realizations in each recording. Fig. 4 shows the aligned and averaged CIRs (truncated to 110 samples) and their path variations. The 3db and Decawave CIRs contain in total 256 and 992 samples, respectively.

Peaks in the CIR correspond to replicas of the signal arriving through multiple paths. Because the pulse bandwidth of 3db devices is significantly lower than the one of Decawave devices ($380\,\mathrm{MHz}$ vs. $662\,\mathrm{MHz}$, respectively), pulses in the 3db CIR are wider. A larger bandwidth increases the time resolution of the device, which improves measurement precision.

The ratio between the amplitude of the first path compared to later replicas is influenced by the RF front-end linearity and therefore depends on the receiver implementation. One class of TOA estimators identifies the maximum-amplitude path and searches backward for the first sample that exceeds the noise floor and is smaller than the maximum amplitude [27]. In NLOS, delayed paths with high amplitudes can produce local minima estimates. Therefore, TOA estimation should take into account NLOS scenarios for the best accuracy.

TABLE II: The useful range of Decawave and 3db devices.

Device	Data rate	Range [m]
3db Access	$247\,\mathrm{kb/s}$	116
Decawave	$110\,\mathrm{kb/s}$	105
Decawave	$6.8\,\mathrm{Mb/s}$	80

C. Distance Measurements

Range: We measured the range of Decawave and 3db devices with no obstruction between the transmitter and the receiver on a marked running track in increments of $5\,\mathrm{m}$. At each point, we recorded the number of timeouts (messages without a response). We define the useful range as the distance at which measurements have less than 10% timeout probability. Both devices use the maximum transmission power within UWB regulations. The range can be extended by increasing the transmission power and tuning the channel and preamble length settings (albeit with higher energy consumption). We also measured the range of Decawave devices in the $6.8\,\mathrm{Mb/s}$ mode. TABLE II shows the measured ranges. The range of 3db devices and Decawave devices in the $110\,\mathrm{kb/s}$ mode exceeds $100\,\mathrm{m}$. The high-rate mode ($6.8\,\mathrm{Mb/s}$) of Decawave has a lower range, of $80\,\mathrm{m}$. Therefore, although the high-rate mode of Decawave reduces the energy consumption, it also decreases the range.

Accuracy and Precision: To characterize distance measurements, we performed an extensive measurement campaign using 3db devices. Because Decawave devices have been included in numerous studies [10]–[12], [15], we rely on already-published results for the comparison. Except for [12], which does not specify the Decawave settings used, all the references use the $110\,\mathrm{kb/s}$ data rate.

Our database includes over 12,000 measurements acquired with the 3db IC in indoor spaces (e.g. large offices, small rooms, and hallways) labeled as either LOS or NLOS, covered in almost equal proportions. To reflect typical real-life situations, we acquired data when devices are stationary or moving at walking speed. In NLOS measurements, the obstruction was caused by the human body, walls, or pillars, out of which the latter two sharply attenuate the direct path. In all NLOS cases, the signal can still arrive at the receiver through reflections—in other words, we did not perform experiments in which the devices are in different rooms.

Since we compare 3db and Decawave devices using measurements obtained in different experiments, there is a chance that the results differ not because of the devices but due to the conditions under which they were acquired (i.e. type of NLOS or multipath environment). On the other hand, this weakness is also a strength, since by relying on Decawave results from more sources, it is more likely that they are more general. When acquiring 3db Access measurements, we strove to recreate all LOS and NLOS conditions considered in the papers which used Decawave devices [10]–[12], [15].

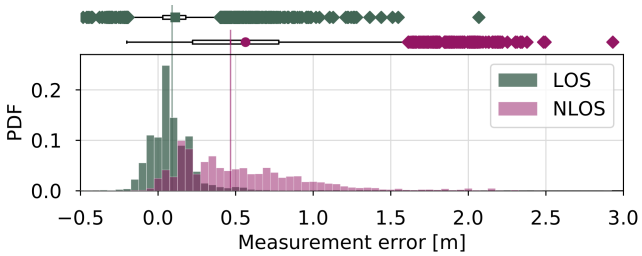

Fig. 5: The PDF and boxplots of LOS and NLOS distance measurements errors of the 3db IC. The median and IQR are, respectively, $9.04\,\mathrm{cm}$ and $14.9\,\mathrm{cm}$ in LOS and $47.74\,\mathrm{cm}$ and $56.3\,\mathrm{cm}$ in NLOS.

TABLE III: Mean and standard deviation of ranging errors in LOS and NLOS with 3db and Decawave devices. We split LOS measurements based on whether the antennas were facing each other or had other poses.

Device		LOS error [cm]		NLOS error [cm]
		Facing antennas	Different antenna poses	
3db Access		4.8 ± 8.4	11 ± 15	62.5 ± 104
Decawave	[10]	4.1 ± 3.2	7.3 ± 3.6*	15.6 ± 7.4*
	[11]	–	0 ± 15	–
	[15]	0.3 ± 5.5	–	34 ± 35

* Average over errors with different antenna poses

Fig. 5 shows the probability distribution function (PDF) of LOS and NLOS errors and TABLE III summarizes their statistics. In Fig. 5, we restricted the domain to $[-0.5, 3]\ \mathrm{m}$ for better visualization but the errors extend up to $19.95\,\mathrm{m}$. Measurements outside the shown boundary occur only in NLOS and represent $0.2\,\%$ of their total. These outliers are caused by a miscalculation of the TOA in NLOS scenarios in the firmware (the issue was later fixed).

In LOS, the irregular radiation pattern of UWB antennas can cause errors up to $\pm 0.4\,\mathrm{m}$ with certain antenna alignments [28]. Therefore, we distinguish measurements where the antennas mounted on the devices were facing each other, which yield the smallest errors, from measurements acquired with other antenna poses. The 3db Access measurements with facing antennas were acquired on a running track (the only outdoor measurements) where we varied the distance between the devices in steps of $8.5\,\mathrm{m}$ up to $51\,\mathrm{m}$. In comparison with Decawave, the ranging accuracy and precision of 3db devices are at most $5.2\,\mathrm{cm}$ higher with the fixed antenna pose and at most $12\,\mathrm{cm}$ higher with different antennas poses.

NLOS scenarios cause the reported distance to be greater or equal than the true one, so the distribution of 3db measurement errors is heavy-tailed and no longer Gaussian-shaped, as shown in Fig. 5. In NLOS, the bias depends on the additional path traveled by the signal and can therefore vary between experiments with different room plans and furnishing. In this case, the error *spread* given by the standard deviation or the interquartile range (IQR) better describes the performance.

In TABLE III, we report the mean and standard deviation of 3db NLOS measurements in order to be consistent with cited Decawave results. However, note that these statistics are shifted upwards because of the infrequent but large outliers, so the median and IQR characterize the distribution more robustly. The IQR of the NLOS error distribution is $56.3\,\mathrm{cm}$. If we eliminate the outliers (which, in a real application, can be filtered out), the standard deviation is halved to $42.57\,\mathrm{cm}$.

The reported NLOS standard deviation of Decawave devices is $35\,\mathrm{cm}$ in office environments [15], between 3.1–$18.7\,\mathrm{cm}$ with human body shadowing [10], and around $20\,\mathrm{cm}$ when the path is blocked by panels made of different materials or concrete walls [12]. NLOS measurements with 3db devices were obtained with *all* these types of obstructions. Therefore, we should compare the 3db error spread with an average over the reported Decawave standard deviations, which is around $20\,\mathrm{cm}$. The IQR of 3db NLOS errors is therefore 2–3 larger than the spread of Decawave errors.

V. Discussion

The results in Section IV warrant a discussion about how the accuracy of distance measurements obtained with the LRP PHY can be improved while still benefiting from the same low energy consumption. We identify several improvements that can be done at the hardware, system, and application level in Sections V-A, V-B, and V-C, respectively.

A. Hardware Improvements

As noted in Section III, 3db devices have almost half the pulse bandwidth of Decawave devices. Since the time resolution of UWB devices is proportional to the pulse bandwidth, increasing the latter could improve the TOA estimation accuracy of 3db devices in both LOS and NLOS conditions.

At the moment, 3db devices can obtain the CIR either from the preamble *or* the postamble for a given measurement. If both CIRs were available at the same time, we could use a similarity metric to detect significant differences in their shape, which usually indicates a highly dynamic environment (i.e. NLOS). Measurements acquired in such conditions could then be discarded or further processed.

In NLOS situations, ranging errors are exacerbated by the clock drift estimation. 3db devices detect the TOA of a packet during the preamble and also during the postamble (at the end of a frame). The clock offset between two devices is computed based on the difference between the two TOAs. Since in NLOS the CIR is highly variable, the postamble TOA might include not only the clock drift error but also a delay caused by the excess path traveled by the signal. In this case, the clock offset estimation will incorrectly compensate for this excess path, increasing the ranging error even more. Discarding measurements in which the postamble and preamble CIRs are very different could therefore reduce the magnitude of NLOS errors, shortening the tail of their PDF.

B. System Improvements

System-level improvements comprise aspects that can be implemented (usually in the firmware) with current hardware capabilities. A firmware issue caused large outliers in 3db measurements acquired in NLOS, which significantly decreased the accuracy and precision of NLOS measurements.

The issue has since been solved, which should show an improvement in future measurements.

As already noted, the multipath components (MPCs) in the CIR significantly affect the TOA estimation. In NLOS, the first path can be very weak (close to the noise floor) and arrive tens of nanoseconds before the strongest MPC [29], so customizing the first path detection algorithm for this scenario could further improve NLOS results.

C. Application Improvements

Localization applications can improve their accuracy through NLOS detection and mitigation techniques using data readily available from the hardware, such as the CIR and its statistics [30]. In addition, filters (e.g. the Extended Kalman Filter) can be used to remove outliers in distance measurements frequently encountered in NLOS situations.

VI. Conclusion

We compared the power and energy consumption and distance measurement statistics of 3db Access and Decawave UWB devices, which implement the LRP and HRP PHYs, respectively. In LOS propagation, 3db devices have slightly higher bias and lower precision than Decawave devices. In NLOS scenarios, the error spread of 3db devices is 2–3 times larger than the one of Decawave. On the other hand, 3db devices have 10x lower average power consumption and 125x lower energy consumption per distance measurement compared to Decawave devices. Therefore, the LRP PHY is suitable for applications which can tolerate a loss in ranging accuracy and precision for higher energy efficiency.

In the future, we will optimize the leading-edge detection of 3db devices to reduce the NLOS error spread and we will integrate the devices in a localization system. The reduced energy consumption can provide location awareness to previously constrained devices (millirobots, body sensors) and generate novel localization applications (for instance, in swarm robotics). It would be interesting to study how the short air time and presumably high device density will impact the access to the medium and the localization update rate of future positioning systems.

References

[1] D. Lymberopoulos and J. Liu, "The Microsoft indoor localization competition: Experiences and lessons learned," *IEEE Signal Processing Magazine*, vol. 34, pp. 125–140, Sept. 2017. Conference Name: IEEE Signal Processing Magazine.

[2] B. Großwindhager, M. Stocker, M. Rath, C. A. Boano, and K. Römer, "SnapLoc: an ultra-fast UWB-based indoor localization system for an unlimited number of tags," in *2019 18th ACM/IEEE International Conference on Information Processing in Sensor Networks (IPSN)*, pp. 61–72, IEEE, 2019.

[3] "Apple U1 TMKA75 ultra wideband (UWB) chip analysis." TechInsights Inc. Report. Accessed on 15-04-2020.

[4] "IEEE 802.15.4z task group." http://www.ieee802.org/15/pub/TG4z.html. Accessed on 15-04-2020.

[5] P. Sedlacek, M. Slanina, and P. Masek, "An overview of the IEEE 802.15. 4z standard its comparison and to the existing UWB standards," in *2019 29th International Conference Radioelektronika (RADIOELEKTRONIKA)*, pp. 1–6, IEEE, 2019.

[6] "IEEE 802.15.4 standard for low-rate wireless networks," 2015.

[7] "Application note APR001. UWB regulations. A summary of worldwide telecommunications regulations governing the use of ultra-wideband radio." Decawave Ltd. Accessed: 15-04-2020.

[8] "Application of IEEE standard 802.15.4," May 2014.

[9] K. Witrisal, G. Leus, G. J. Janssen, M. Pausini, F. Troesch, T. Zasowski, and J. Romme, "Noncoherent ultra-wideband systems," *IEEE Signal Processing Magazine*, vol. 26, pp. 48–66, July 2009. Conference Name: IEEE Signal Processing Magazine.

[10] Q. Tian, K. I.-K. Wang, and Z. Salcic, "Human body shadowing effect on UWB-based ranging system for pedestrian tracking," *IEEE Transactions on Instrumentation and Measurement*, vol. 68, pp. 4028–4037, Oct. 2019. Conference Name: IEEE Transactions on Instrumentation and Measurement.

[11] B. J. Silva and G. P. Hancke, "Ranging error mitigation for through-the-wall non-line-of-sight conditions," *IEEE Transactions on Industrial Informatics*, pp. 1–1, 2020. Conference Name: IEEE Transactions on Industrial Informatics.

[12] A. Schenck, E. Walsh, J. Reijniers, T. Ooijevaar, R. Yudanto, E. Hostens, W. Daems, and J. Steckel, "Information theoretic framework for the optimization of UWB localization systems," in *2018 International Conference on Indoor Positioning and Indoor Navigation (IPIN)*, pp. 1–8, Sept. 2018. ISSN: 2471-917X.

[13] "DW1000 user manual. Version 2.11." Decawave Ltd.

[14] A. R. J. Ruiz and F. S. Granja, "Comparing Ubisense, Bespoon, and Decawave UWB location systems: Indoor performance analysis," *IEEE Transactions on instrumentation and Measurement*, vol. 66, no. 8, pp. 2106–2117, 2017.

[15] A. R. Jiménez and F. Seco, "Comparing Decawave and Bespoon UWB location systems: Indoor/outdoor performance analysis," in *2016 International Conference on Indoor Positioning and Indoor Navigation (IPIN)*, pp. 1–8, IEEE, 2016.

[16] J. Wang, A. K. Raja, and Z. Pang, "Prototyping and experimental comparison of IR-UWB based high precision localization technologies," in *UIC-ATC-ScalCom*, pp. 1187–1192, IEEE, 2015.

[17] "3db Access." www.3db-access.com. Accessed on 15-04-2020.

[18] F. C. Commission *et al.*, "Revision of part 15 of the commission's rules regarding ultra-wideband transmission systems," *First Report and Order, FCC 02-48*, 2002.

[19] M. Weisenhorn and W. Hirt, "Robust noncoherent receiver exploiting UWB channel properties," in *2004 International Workshop on Ultra Wideband Systems Joint with Conference on Ultra Wideband Systems and Technologies. Joint UWBST & IWUWBS 2004 (IEEE Cat. No. 04EX812)*, pp. 156–160, IEEE, 2004.

[20] H. Arslan, Z. N. Chen, and M.-G. Di Benedetto, *Ultra wideband wireless communication*. John Wiley & Sons, 2006.

[21] J. G. Proakis and M. Salehi, *Digital communications*, vol. 4. McGraw-hill New York, 2001.

[22] S. Gezici, Z. Tian, G. B. Giannakis, H. Kobayashi, A. F. Molisch, H. V. Poor, and Z. Sahinoglu, "Localization via ultra-wideband radios: A look at positioning aspects for future sensor networks," *IEEE signal processing magazine*, vol. 22, no. 4, pp. 70–84, 2005.

[23] I. Guvenc, C.-C. Chong, and F. Watanabe, "Analysis of a linear least-squares localization technique in los and nlos environments," in *2007 IEEE 65th Vehicular Technology Conference-VTC2007-Spring*, pp. 1886–1890, IEEE, 2007.

[24] D. Neirynck, E. Luk, and M. McLaughlin, "An alternative double-sided two-way ranging method," in *2016 13th workshop on positioning, navigation and communications (WPNC)*, pp. 1–4, IEEE, 2016.

[25] "Ranging demo user guide. Understanding and using the DecaRanging ranging demo (PC) application. Version 4.5." Decawave Ltd.

[26] "DW1000 datasheet. Version 2.09." Decawave Ltd.

[27] H. Soganci, S. Gezici, and H. V. Poor, "Accurate positioning in ultra-wideband systems," *IEEE Wireless Communications*, vol. 18, no. 2, pp. 19–27, 2011.

[28] A. Ledergerber and R. D'andrea, "Calibrating away inaccuracies in ultra wideband range measurements: A maximum likelihood approach," *IEEE Access*, vol. 6, pp. 78719–78730, 2018. IEEE Access.

[29] Z. Sahinoglu, S. Gezici, and I. Guvenc, "Ultra-wideband positioning systems," *Cambridge, New York*, 2008.

[30] J. Khodjaev, Y. Park, and A. Saeed Malik, "Survey of NLOS identification and error mitigation problems in UWB-based positioning algorithms for dense environments," *Annals of telecommunications*, vol. 65, pp. 301–311, June 2010.